

We have demonstrated that $\text{Ru}(\text{CO})_3(\text{C}_2\text{H}_4)_2$ not only is a catalyst for alkene isomerization¹ but also serves as a "Ru(CO)₃" transfer reagent, permitting the synthesis of novel, thermally labile ruthenium complexes of acyclic nonconjugated dienes.

Acknowledgment. We thank the National Science Foundation and the Office of Naval Research for support of this work.

Registry No. $\text{Ru}_3(\text{CO})_{12}$, 15243-33-1; $\text{Ru}(\text{CO})_3(\text{PPh}_3)_2$, 14741-36-7; $\text{Ru}(\text{CO})_3(\text{C}_2\text{H}_4)$, 115512-39-5; $\text{Ru}(\text{CO})_4(\text{C}_2\text{H}_4)$, 52621-15-5; $\text{Ru}(\text{C}_2\text{O})_4(\text{C}_3\text{H}_6)$, 106520-68-7; $\text{Ru}(\text{CO})_4(\text{C}_5\text{H}_{10})$, 67606-17-1; $\text{Ru}(\text{CO})_4(\eta^2-1,4\text{-pentadiene})$, 115512-40-8; $\text{Ru}(\text{CO})_4(\eta^2-3\text{-Me-1,4-C}_5\text{H}_7)$, 115512-41-9; $\text{Ru}(\text{CO})_4(\eta^2-1,5\text{-hexadiene})$, 115512-42-0; $\text{Ru}(\text{CO})_4(\eta^2-1,6\text{-heptadiene})$, 115512-43-1; $\text{Ru}(\text{CO})_3(\text{C}_2\text{H}_4)_2$, 106520-58-5; $\text{Ru}(\text{CO})_3(\text{C}_3\text{H}_6)_2$,

106520-70-1; $\text{Ru}(\text{CO})_3(\text{C}_5\text{H}_{10})_2$, 106520-67-6; $\text{Ru}(\text{CO})_3(\eta^2-1,4\text{-pentadiene})_2$, 115512-44-2; $\text{Ru}(\text{CO})_3(\eta^2-1,6\text{-heptadiene})_2$, 115512-45-3; $\text{Ru}(\text{CO})_3(\eta^2-1,4\text{-pentadiene})$, 115512-46-4; $\text{Ru}(\text{CO})_3(\eta^2-3\text{-Me-1,4-C}_5\text{H}_7)$, 115512-47-5; $\text{Ru}(\text{CO})_3(\eta^2-1,5\text{-hexadiene})$, 115512-48-6; $\text{Ru}(\text{CO})_3(\eta^2-1,3\text{-pentadiene})$, 106621-53-8; $\text{Ru}(\text{CO})_3(\eta^2-3\text{-Me-1,3-C}_5\text{H}_7)$, 115512-49-7; $\text{Ru}(\text{CO})_3(\eta^2-1,3\text{-butadiene})$, 62883-45-8; $\text{HRu}(\text{CO})_3(\eta^3\text{-C}_3\text{H}_5)$, 106520-69-8; $\text{HRu}(\text{CO})_3(\eta^3\text{-C}_5\text{H}_9)$, 106520-72-3; $\text{HRu}(\text{CO})_3(\eta^3\text{-C}_5\text{H}_7)$, 115512-50-0.

Supplementary Material Available: Two figures showing IR spectral changes for $\text{Ru}(\text{CO})_4(\eta^2-1,5\text{-hexadiene})$ flash photolysis in the presence of 1,5-hexadiene forming $\text{Ru}(\text{CO})_3(\eta^2-1,5\text{-hexadiene})$ and for thermal reaction of $\text{Ru}(\text{CO})_3(\text{C}_2\text{H}_4)_2$ with 1,6-heptadiene forming $\text{Ru}(\text{CO})_3(\eta^2-1,6\text{-heptadiene})_2$ (2 pages). Ordering information is given on any current masthead page.

Contribution from the Department of Chemistry,
University of Arizona, Tucson, Arizona 85721

Synthesis, Characterization, and Oxygen Atom Transfer Reactions of $\{\text{HB}(\text{Me}_2\text{C}_3\text{N}_2\text{H})_3\}\text{MoO}\{\text{S}_2\text{P}(\text{OR})_2\}$ and $\{\text{HB}(\text{Me}_2\text{C}_3\text{N}_2\text{H})_3\}\text{MoO}_2\{\eta^1\text{-S}_2\text{P}(\text{OEt})_2\}$

Sue A. Roberts, Charles G. Young, W. E. Cleland, Jr., Richard B. Ortega, and John H. Enemark*

Received August 26, 1987

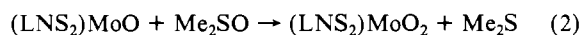
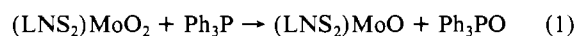
The compounds $\{\text{HB}(\text{Me}_2\text{pz})_3\}\text{MoO}\{\text{S}_2\text{P}(\text{OEt})_2\}$ (**1a**) and $\{\text{HB}(\text{Me}_2\text{pz})_3\}\text{MoO}_2\{\text{S}_2\text{P}(\text{OEt})_2\}$ (**2**) containing bidentate and monodentate $\text{S}_2\text{P}(\text{OEt})_2^-$ ligands, respectively, have been prepared by the reaction of $\text{Mo}_2\text{O}_3\{\text{S}_2\text{P}(\text{OEt})_2\}_4$ with $\text{K}\{\text{HB}(\text{Me}_2\text{pz})_3\}$. $\{\text{HB}(\text{Me}_2\text{pz})_3\}\text{MoO}\{\text{S}_2\text{P}(\text{OEt})_2\}$ and its analogue $\{\text{HB}(\text{Me}_2\text{pz})_3\}\text{MoO}\{\text{S}_2\text{P}(\text{OMe})_2\}$ have also been prepared in higher yield by the reaction of $\text{Mo}_2\text{O}_3\{\text{S}_2\text{P}(\text{OEt})_2\}_4$ with Ph_3P followed by reaction with $\text{K}\{\text{HB}(\text{Me}_2\text{pz})_3\}$. Both **1a** and **2** have been structurally characterized by X-ray crystallography. The blue Mo(IV) compound **1a** crystallizes in the monoclinic space group $P2_1/c$ with $a = 17.987$ (3) Å, $b = 8.219$ (3) Å, $c = 18.681$ (7) Å, $\beta = 104.88$ (2)°, and $Z = 4$. The molybdenum atom is six-coordinate and facially coordinated by the tridentate $\text{HB}(\text{Me}_2\text{pz})_3^-$ ligand, by one terminal oxo ligand ($\text{Mo}=\text{O} = 1.644$ (6) Å) and by the bidentate $\text{S}_2\text{P}(\text{OEt})_2^-$ ligand. The gold-colored Mo(VI) complex **2** crystallizes as the toluene hemisolvate in the triclinic space group $P\bar{1}$ with $a = 8.421$ (1) Å, $b = 12.654$ (6) Å, $c = 15.240$ (5) Å, $\alpha = 87.77$ (3)°, $\beta = 81.36$ (2)°, $\gamma = 74.37$ (3)°, and $Z = 2$. The molybdenum atom is six-coordinate with a tridentate $\text{HB}(\text{Me}_2\text{pz})_3^-$ ligand, two terminal oxo ligands ($\text{Mo}=\text{O} = 1.690$ (2) and 1.697 (2) Å), and a monodentate $\text{S}_2\text{P}(\text{OEt})_2^-$ ligand. The $\text{S}_2\text{P}(\text{OEt})_2^-$ ligand adopts an extended geometry, and the uncoordinated sulfur atom is 5.42 Å from the molybdenum atom. Compound **1a** reduces Me_2SO to Me_2S . The kinetic data can be fit to a second-order rate law with $k = 5.46$ (6) $\times 10^{-5}$ (M s)⁻¹ in toluene at 40 °C. Activation parameters determined from plots of $\ln(k/T)$ vs $1/T$ are $\Delta H^\ddagger = 15.3$ (2) kcal mol⁻¹ and $\Delta S^\ddagger = -29$ (2) cal (mol K)⁻¹. The large negative entropy of activation indicates that an associative mechanism is operative. Compound **2** oxidizes Ph_3P to Ph_3PO . Again, a second-order rate law is followed; $k = 3.4$ (1) $\times 10^{-3}$ (M s)⁻¹ in toluene at 25 °C. Both complexes catalyze the oxidation of Ph_3P by Me_2SO .

Introduction

Considerable recent research has been directed toward the preparation of mononuclear high-valent oxomolybdenum complexes as structural and reactivity models of the molybdenum site in oxo-type molybdoenzymes.¹ These enzymes catalyze net oxygen atom transfer reactions, as typified by the oxidation of sulfite to sulfate (sulfite oxidase) or the oxidation of xanthine to uric acid (xanthine oxidase).² Recently, Hille and Sprecher³ have shown that the oxygen atom added to xanthine by xanthine oxidase arises from the molybdenum complex exclusively and not from a solvent molecule. Several oxomolybdenum(IV) and oxomolybdenum(VI) complexes containing sulfur-donor ligands are known to undergo oxygen atom transfer reactions.⁴ The well-known complex $\text{MoO}_2(\text{S}_2\text{CNEt}_2)_2$ undergoes facile oxygen atom transfer reactions⁵ but is unsuitable as a model system for oxo-type

molybdoenzymes because a stable oxo-bridged dimer readily forms in solution.⁶ In general, comproportionation of molybdenum(IV) and molybdenum(VI) complexes to form stable dinuclear complexes, a common reaction in oxomolybdenum chemistry, must be inhibited to achieve a catalytic cycle.

Berg and Holm⁷ have synthesized a five-coordinate dioxomolybdenum(VI) complex containing the 2,6-bis-(2,2-diphenyl-2-mercaptoethyl)pyridine ligand (LNS_2) in which phenyl rings adjacent to the ligating sulfur atoms provide steric hindrance and prevent dimerization upon reduction. The dioxomolybdenum(VI) complex of LNS_2 transfers an oxygen atom to triphenylphosphine (eq 1) to generate an oxo-Mo(IV) complex, which can in turn be reoxidized by an oxygen atom abstraction reaction with Me_2SO (eq 2). Coupling of reactions 1 and 2 results in the catalytic



transfer of an oxygen atom from Me_2SO to Ph_3P , a reaction that does not proceed in the absence of a catalyst. These complexes and others⁸ that have been reported to catalyze this reaction cycle

- Garner, C. D.; Bristow, S. In *Molybdenum Enzymes*; Spiro, T. G., Ed.; Wiley: New York, 1985; pp 343-410.
- Hille, R.; Massey, V. In *Molybdenum Enzymes*; Spiro, T. G., Ed.; Wiley: New York, 1985; pp 443-518.
- Hille, R.; Sprecher, H. *J. Biol. Chem.* **1987**, *262*, 10914-10917.
- Topich, J.; Lyon, J. T. *Inorg. Chim. Acta* **1983**, *80*, L41-43. Topich, J.; Lyon, J. T. *Polyhedron* **1984**, *3*, 61-65. Speier, G. *Inorg. Chim. Acta* **1979**, *32*, 139-141. Nicholas, K. M.; Khan, M. A. *Inorg. Chem.* **1987**, *26*, 1633-1636.
- Newton, W. E.; Corbin, J. L.; Bravard, D.; Searles, J. E.; McDonald, J. *Inorg. Chem.* **1974**, *13*, 1100. Mitchell, P. C. H.; Scarle, R. *J. Chem. Soc., Dalton Trans.* **1975**, 2552-2555. Durant, R.; Garner, C. D.; Hyde, M. R.; Mabbs, F. E. *J. Chem. Soc., Dalton Trans.* **1977**, 955-956.

(6) Reynolds, M. S.; Berg, J. M.; Holm, R. H. *Inorg. Chem.* **1984**, *23*, 3057-3062.

(7) Holm, R. H.; Berg, J. M. *Acc. Chem. Res.* **1986**, *19*, 363-370. Harlan, E. W.; Berg, J. M.; Holm, R. H. *J. Am. Chem. Soc.* **1986**, *108*, 6992-7000. Berg, J. M.; Holm, R. H. *J. Am. Chem. Soc.* **1985**, *107*, 925-932.

are similar in that they contain sulfur-donor ligands and their Mo(IV) complexes either are five-coordinate with a vacant coordination site or contain a dissociable coordinated solvent.

We have previously reported the use of the ligand hydrotris-(3,5-dimethyl-1-pyrazolyl)borate ($\text{HB}(\text{Me}_2\text{pz})_3^-$) to prepare stable, mononuclear molybdenum(IV) and molybdenum(V) complexes.⁹⁻¹¹ The facial coordination of this ligand ensures that all other ligands will have mutually cis stereochemistry and that the complexes will be restricted to being six-coordinate. In addition, the steric constraints of the methyl groups on the pyrazole rings prevent formation of oxo-bridged dimers under most circumstances. Oxomolybdenum compounds of $\text{HB}(\text{Me}_2\text{pz})_3^-$ containing sulfur ligands provide a coordination sphere whose electronic properties are similar to those proposed for oxomolybdenum enzymes.¹⁰ Herein we show that oxomolybdenum complexes stabilized by the $\text{HB}(\text{Me}_2\text{pz})_3^-$ ligand also function as rudimentary reactivity models for oxo-transfer reactions of enzyme active sites. The complexes $\{\text{HB}(\text{Me}_2\text{pz})_3\}\text{MoO}_2\{\text{S}_2\text{P}(\text{OEt})_2\}$ (**1a**) and $\{\text{HB}(\text{Me}_2\text{pz})_3\}\text{MoO}_2\{\text{S}_2\text{P}(\text{OEt})_2\}$ (**2**) catalyze the reactions of eq 1 and 2 without formation of oxo-bridged dimers.¹²

Experimental Section

Materials and Methods. Potassium hydrotris(3,5-dimethyl-1-pyrazolyl)borate¹³ was prepared by literature methods. All reactions were performed under an atmosphere of pure dinitrogen with use of dried and deoxygenated solvents. Infrared spectra were recorded on a Perkin-Elmer 983 spectrophotometer as KBr disks. ¹H, ³¹P, and ⁹⁵Mo NMR spectra were recorded on a Bruker WM250 spectrometer. Chemical shifts were referenced to internal TMS, external 85% H_3PO_4 , and external 2 M $\text{Na}_2\text{MoO}_4/\text{D}_2\text{O}$ (pH 11), respectively (positive chemical shifts are deshielded relative to the reference). The electronic spectra were recorded on an IBM 9420 spectrophotometer using quartz cells. Electrochemical experiments were performed at a glassy-carbon electrode on an IBM EC225 voltammetric analyzer using 1 mM acetonitrile solutions of the complexes and 0.1 M Bu_4NBF_4 as supporting electrolyte. Potentials are reported relative to 0.1 M Ag/AgNO_3 in MeCN.

Preparation of Compounds. (μ -Oxo)bis(oxo(dialkyl dithiophosphato)molybdenum(V)), $\text{Mo}_2\text{O}_3\{\text{S}_2\text{P}(\text{OR})_2\}_4$ (**R = Et, Me**). These compounds were prepared by a modification of the literature method.¹⁴ A solution of $\text{NH}_4\{\text{S}_2\text{P}(\text{OR})_2\}$ (54.9 mmol) in water (60 mL) was slowly added to a stirred solution of MoCl_5 (5 g, 18.3 mmol) in 6 M HCl (30 mL). The purple precipitate was collected by filtration, washed thoroughly with water and then ethanol, and dried in air. The crude product was dissolved in toluene, and the solution was filtered and evaporated to dryness in vacuo. The purple microcrystalline product was washed with hexanes, dried in vacuo, and stored under nitrogen. The yield was 50–80% over several preparations.

Oxo{hydrotris(3,5-dimethyl-1-pyrazolyl)borato}{dialkyl dithiophosphato)molybdenum(IV), $\{\text{HB}(\text{Me}_2\text{pz})_3\}\text{MoO}\{\text{S}_2\text{P}(\text{OR})_2\}$ (**R = Et (1a), Me (1b)**). A mixture of $\text{Mo}_2\text{O}_3\{\text{S}_2\text{P}(\text{OR})_2\}_4$ (2.0 mmol) and Ph_3P (0.525 g, 2.0 mmol) in toluene (50 mL) was refluxed for 1 h. When the mixture was cooled, $\text{K}\{\text{HB}(\text{Me}_2\text{pz})_3\}$ (1.48 g, 4.4 mmol) was added and the mixture was refluxed for a further 4 h. The cooled suspension was filtered in air and the solvent removed in vacuo. The blue complex was isolated by column chromatography on silica gel with use of dichloromethane as solvent and recrystallized from dichloromethane/methanol. Yields: **1a**, 1.8 g (71%); **1b**, 1.6 g (66%).

Physical Data for 1a. Anal. Calcd for $\text{C}_{19}\text{H}_{32}\text{BMoN}_6\text{O}_3\text{PS}_2$: C, 38.39; H, 5.43; N, 14.40; S, 10.79. Found: C, 38.5; H, 5.5; N, 14.3; S, 11.0. Infrared spectrum (cm^{-1}): $\nu(\text{BH})$ 2543 m, $\nu(\text{Mo}=\text{O})$ 962 s. ¹H NMR (CDCl_3 , δ): 1.34 and 1.50 (t, $J = 7.0$ Hz, 2×3 H, CH_3 of $\text{S}_2\text{P}(\text{OEt})_2^-$); 2.20 and 2.21 (s, 2×3 H, CH_3 of $\text{HB}(\text{Me}_2\text{pz})_3^-$); 2.45 and 2.69 (s, 2×3 H, CH_3 of $\text{HB}(\text{Me}_2\text{pz})_3^-$); 4.21 and 4.45 (dq, $J_{\text{H-H}} = 7.0$ Hz, $J_{\text{H-P}} = 7.1$ Hz, 2×2 H, CH_2); 5.45 (s, 1 H, CH); 6.00 (s, 2 H, CH).

³¹P{¹H} NMR (CDCl_3 , δ): 135.4. ⁹⁵Mo NMR (CH_2Cl_2 , δ): 2950 ($w_{1/2} = 1750$ Hz). Electronic spectrum (CH_2Cl_2 ; λ , nm (ϵ)): 642 (100); 382 (80). Electrochemistry: quasi-reversible oxidation at 0.68 V.

Physical Data for 1b. Anal. Calcd for $\text{C}_{19}\text{H}_{32}\text{BMoN}_6\text{O}_3\text{PS}_2$: C, 36.05; H, 4.98; N, 14.84; S, 11.32. Found: C, 35.9; H, 5.0; N, 14.8; S, 11.3. Infrared spectrum (cm^{-1}): $\nu(\text{BH})$ 2533 m, $\nu(\text{Mo}=\text{O})$ 956 s. ¹H NMR (CDCl_3 , δ): 2.17 and 2.21 (s, 2×3 H, CH_3 of $\text{HB}(\text{Me}_2\text{pz})_3^-$); 2.46 and 2.70 (s, 2×6 H, CH_3 of $\text{HB}(\text{Me}_2\text{pz})_3^-$); 3.87 and 4.02 (d, $J_{\text{H-P}} = 13.5$ Hz, 2×3 H, CH_3 of $\text{S}_2\text{P}(\text{OMe})_2^-$); 5.45 (s, 1 H, CH); 6.00 (s, 2 H, CH). ³¹P NMR (CDCl_3 , δ): 136.97 (septet, $J_{\text{P-H}} = 13.5$ Hz). ⁹⁵Mo NMR (CH_2Cl_2 , δ): 2930 ($w_{1/2} = 2440$ Hz). Electrochemistry: quasi-reversible oxidation at 0.61 V.

cis-Dioxo{hydrotris(3,5-dimethyl-1-pyrazolyl)borato}{diethyl dithiophosphato)molybdenum(VI), $\{\text{HB}(\text{Me}_2\text{pz})_3\}\text{MoO}_2\{\text{S}_2\text{P}(\text{OEt})_2\}$ (**2**). A mixture of $\text{K}\{\text{HB}(\text{Me}_2\text{pz})_3\}$ (0.7 g, 2.08 mmol) and $\text{Mo}_2\text{O}_3\{\text{S}_2\text{P}(\text{OEt})_2\}_4$ (1.0 g, 1.0 mmol) in toluene (60 mL) was heated at 60 °C for 1.5 h. The brown mixture was evaporated to dryness, the residue was redissolved in CH_2Cl_2 , and the solution was then chromatographed on silica gel with use of the same solvent. Following the elution of the blue band (**1a**), the yellow band, $\{\text{HB}(\text{Me}_2\text{pz})_3\}\text{MoO}_2\{\text{S}_2\text{P}(\text{OEt})_2\}$ (**2**), was collected and evaporated to dryness. The compound was recrystallized by slow cooling from toluene solution and dried in a vacuum oven. The yield was 0.22 g (34%).

Physical Data for 2. Anal. Calcd for $\text{C}_{19}\text{H}_{32}\text{BMoN}_6\text{O}_4\text{PS}_2$: C, 37.39; H, 5.28; N, 13.77. Found: C, 37.42; H, 5.29; N, 13.75. Infrared spectrum (cm^{-1}): $\nu(\text{BH})$ 2548 m, $\nu(\text{Mo}=\text{O})$ 933 s, 900 s. ¹H NMR (CDCl_3 , δ): 1.39 (t, $J = 7.0$ Hz, 2×3 H, CH_3 of $\text{S}_2\text{P}(\text{OEt})_2^-$); 2.34 and 2.37 (s, 2×3 H, CH_3 of $\text{HB}(\text{Me}_2\text{pz})_3^-$); 2.58 and 2.76 (s, 2×3 H, CH_3 of $\text{HB}(\text{Me}_2\text{pz})_3^-$); 4.30 (2×2 H, CH_2 of $\text{S}_2\text{P}(\text{OEt})_2^-$); 5.84 (s, 3 H, CH of $\text{HB}(\text{Me}_2\text{pz})_3^-$); 7.25 and 2.68 (toluene solvate). ³¹P{¹H} NMR ($\text{CH}_2\text{Cl}_2/\text{CDCl}_3$, δ): 95.75. ⁹⁵Mo NMR (CH_2Cl_2 , δ): 162 ($w_{1/2} = 340$ Hz). Electronic spectrum (CH_2Cl_2 ; λ , nm (ϵ)): 340 (6080). Electrochemistry: all waves irreversible; peak currents at -0.50, -0.90, and +0.75 V.

Kinetics Measurements. Reactions were followed spectrophotometrically with use of an IBM 9420 UV-visible spectrophotometer and quartz cells. Solutions were equilibrated at the specified temperature prior to use. All reactions were run under pseudo-first-order conditions with $[\text{reactant}]/[\text{Mo complex}]$ ranging from 10/1 to 200/1. The initial concentration of molybdenum complex was 3.5 mM. Solutions of **2** decompose significantly overnight and were prepared fresh daily. Solutions of **1a** are stable for several weeks, and no such precautions were necessary.

Structure Determinations. Crystal data for **1a** and **2**·0.5tol (tol = toluene) and details of the structure determinations are given in Table I. Intensity data were collected on a Syntex P2₁ diffractometer running locally modified P3 software. Absorption corrections were not made; absorption coefficients, as shown in Table I, are small. In neither case was a decay correction necessary. For both structures, scattering factors were taken from Cromer and Waber.¹⁵ Anomalous dispersion effects were included for all non-hydrogen atoms; the values were those of Cromer.¹⁶ All calculations were performed on a PDP-11/34a computer using SDP-Plus.¹⁷

For **1a**, the position of the molybdenum atom was determined from a Patterson map. All other non-hydrogen atoms were found in succeeding difference electron density maps. Hydrogen atoms were added to the structure at calculated positions but not refined. Because of the scarcity of data (reflections were observed only to $2\theta = 40^\circ$), only Mo, S, and P atoms were refined anisotropically. Final R values for refinement of 153 variables and 1570 reflections with $F_o^2 > 3\sigma(F_o^2)$ were $R = 0.051$ and $R_w = 0.058$. Final positional and equivalent isotropic thermal parameters for all refined atoms are given in Table II.

For **2**, the position of the molybdenum atom was determined from a Patterson map. Other non-hydrogen atoms were found in succeeding difference electron density maps. After all the atoms in the complex had been located, a smear of electron density remained about the inversion center at $0, 1/2, 1/2$. The size and shape of the residual electron density resembled that of a toluene molecule, but all atomic positions were not resolved. A toluene molecule was added to the structure at this position with B set to 14.0 for each atom. Since $\bar{1}$ symmetry is required, the methyl group carbon atom was included at half-occupancy, disordered between bonding to C(1) and C(1)'. Positional and thermal parameters

- (8) Kaul, B. B.; Enemark, J. H.; Merbs, S. L.; Spence, J. T. *J. Am. Chem. Soc.* **1985**, *107*, 2885–2891.
- (9) Young, C. G.; Roberts, S. A.; Ortega, R. B.; Enemark, J. H. *J. Am. Chem. Soc.* **1987**, *109*, 2938–2946.
- (10) Cleland, W. E., Jr.; Barnhart, K. M.; Yamanouchi, K.; Collison, D.; Mabbs, F. E.; Ortega, R. B.; Enemark, J. H. *Inorg. Chem.* **1987**, *26*, 1017–1025.
- (11) Young, C. G.; Enemark, J. H.; Collison, D.; Mabbs, F. E. *Inorg. Chem.* **1987**, *26*, 2925–2927.
- (12) Presented in part at the 192nd National Meeting of the American Chemical Society, Anaheim, CA, Sept 1986, paper INOR 240.
- (13) Trofimenko, S. *J. Am. Chem. Soc.* **1967**, *89*, 6288–6294.
- (14) Jowitt, R. N.; Mitchell, P. C. H. *J. Chem. Soc. A* **1970**, 1702–1708.

- (15) Cromer, D. T.; Waber, J. T. In *International Tables for X-Ray Crystallography*; Kynoch: Birmingham, England, 1974; Vol. IV, Table 2.2B.
- (16) Cromer, D. T. In *International Tables for X-Ray Crystallography*; Kynoch: Birmingham, England, 1974; Vol. IV, Table 2.3.1.
- (17) Frenz, B. A. In *Computing in Crystallography*; Schenck, H., Othof-Hazelkamp, R., van Koningsveld, H., Bassi, G. C., Eds.; Delft University Press: Delft, The Netherlands, 1978; pp 64–71.

Table I. Experimental Details for the Structure Determinations

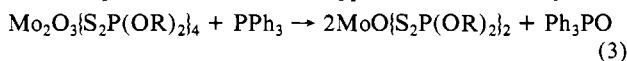
	1a	2
A. Crystal Data		
chem formula	MoS ₂ PO ₃ N ₆ C ₁₉ BH ₃₂	MoS ₂ PO ₄ N ₆ C ₁₉ BH ₃₂ ^a 1/2C ₇ H ₈
cryst color	blue	golden yellow
cryst size, mm	0.5 × 0.17 × 0.06	cryst lost
ω-scan width, deg	0.4	0.35
radiation	Mo Kα (λ = 0.71073 Å), Nb filtered	Mo Kα (λ = 0.71073 Å), graphite monochromated
temp, °C	23 ± 1	23 ± 1
space group,	P2 ₁ /c, monocl	P1̄, tricl
cryst class		
cell params		
a, Å	17.987 (3)	8.421 (1)
b, Å	8.219 (3)	12.654 (6)
c, Å	18.681 (7)	15.240 (5)
α, deg	90.0	87.77 (3)
β, deg	104.88 (2)	81.36 (2)
γ, deg	90.0	74.37 (3)
cell vol, Å ³	2669	1546
Z	4	2
ρ _{calcd} , ρ _{meas} , g cm ⁻³	1.48, 1.49	1.43, 1.40
μ, cm ⁻¹	7.2	6.3
B. Intensity Measurements		
scan type	θ-2θ	θ-2θ
scan rate, deg min ⁻¹	variable, 2-8	variable, 3-30
scan width, deg	(Kα ₁ - 1.0) - (Kα ₂ + 1.4)	(Kα ₁ - 1.1) - (Kα ₂ + 1.2)
2θ _{max} , deg	40	45
rflns collected	±h,k,l	h,±k,±l
no. of rflns (total, unique)	2833, 2388	4730, 4062
corrections	Lp	Lp
rfln av (R _{int})	2.1	0.8
C. Solution and Refinement		
rflns used	1570	3531
F _o ² > 3σ(F _o ²) ^a		
least-squares wts	4F _o ² /σ ² (F _o ²)	
p	0.04	0.03
no. of params	153	307
R ^b	0.051	0.043
R _w ^c	0.058	0.064
GOF ^c	1.49	3.19
(Δ/σ) _{max}	0.01	0.07
Δρ _{max} (vicinity), e Å ⁻³	1.07 (Mo)	1.35 (solvent)

^aσ²(F_o²) = (σ²(I) + (pF_o²)²). ^bR = (Σ||F_o - |F_c||/Σ|F_o|). ^cR_w = [Σw(|F_o - |F_c||)²/ΣwF_o²]^{1/2}. ^dGOF = [(Σw|F_o - |F_c||²)/(N_o - N_c)]^{1/2}.

of the solvent atoms were not refined. Hydrogen atoms were added to the structure at calculated positions and restrained to ride on the atoms to which they were bonded. Hydrogen atoms on the solvent molecule were not included in the calculations. Final R values for refinement of 307 variables and 3531 reflections with F_o² > 3σ(F_o²) were R = 0.043 and R_w = 0.064. Final positional and equivalent isotropic thermal parameters for all refined atoms are given in Table III.

Results and Discussion

Syntheses. The blue complexes [HB(Me₂pz)₃]MoO[S₂P(OR)₂]₂, (**1a**, **1b**) can be prepared in about 70% yield from the reaction of K[HB(Me₂pz)₃] with the known MoO[S₂P(OR)₂]₂ complexes,¹⁸ which have been generated via the oxygen atom transfer reactions shown in eq 3.¹⁹ Solid **1a** and **1b** appear to be indefinitely stable



in air; however, slow oxidation of **1b** was observed in solution. This method of preparation parallels the convenient preparation of

Table II. Positional Parameters for [HB(Me₂pz)₃]MoO[S₂P(OEt)₂]^a

atom	x	y	z	B _{eq} , Å ²
Mo	0.27993 (6)	0.1503 (1)	0.22757 (5)	2.24 (2)
S(1)	0.1518 (2)	0.2716 (4)	0.2189 (2)	3.64 (8)
S(2)	0.2213 (2)	-0.0680 (4)	0.2887 (2)	3.34 (7)
P	0.1424 (2)	0.0992 (4)	0.2911 (2)	3.03 (8)
O(1)	0.3313 (4)	0.242 (1)	0.3023 (4)	3.3 (2)*
O(2)	0.0619 (4)	0.013 (1)	0.2742 (4)	3.7 (2)*
O(3)	0.1520 (4)	0.184 (1)	0.3681 (4)	4.0 (2)*
N(11)	0.2273 (5)	0.018 (1)	0.1077 (5)	2.4 (2)*
N(12)	0.2731 (5)	0.021 (1)	0.0591 (4)	2.3 (2)*
N(21)	0.3777 (4)	0.009 (1)	0.2135 (4)	2.1 (2)*
N(22)	0.4009 (5)	0.018 (1)	0.1486 (4)	2.3 (2)*
N(31)	0.3086 (5)	0.328 (1)	0.1533 (4)	2.4 (2)*
N(32)	0.3415 (5)	0.285 (1)	0.0975 (4)	2.3 (2)*
C(11)	0.1642 (7)	-0.062 (2)	0.0721 (6)	3.5 (3)*
C(12)	0.1707 (7)	-0.110 (1)	0.0044 (6)	3.5 (3)*
C(13)	0.2379 (6)	-0.054 (2)	-0.0046 (6)	3.3 (3)*
C(14)	0.0979 (8)	-0.095 (2)	0.1048 (8)	5.5 (4)*
C(15)	0.2723 (8)	-0.070 (2)	-0.0681 (7)	4.9 (3)*
C(21)	0.4306 (6)	-0.081 (1)	0.2611 (6)	2.4 (2)*
C(22)	0.4863 (6)	-0.129 (2)	0.2271 (6)	3.5 (3)*
C(23)	0.4662 (6)	-0.066 (1)	0.1566 (6)	2.5 (2)*
C(24)	0.4272 (7)	-0.112 (2)	0.3374 (6)	4.0 (3)*
C(25)	0.5071 (7)	-0.084 (2)	0.0965 (7)	4.8 (3)*
C(31)	0.3069 (6)	0.492 (1)	0.1538 (6)	2.9 (2)*
C(32)	0.3368 (7)	0.548 (2)	0.0993 (6)	3.7 (3)*
C(33)	0.3569 (6)	0.419 (1)	0.0622 (6)	2.9 (3)*
C(34)	0.2806 (8)	0.585 (2)	0.2093 (7)	5.1 (3)*
C(35)	0.3921 (7)	0.415 (2)	-0.0020 (7)	4.6 (3)*
C(41)	-0.0097 (7)	0.106 (2)	0.2713 (6)	4.3 (3)*
C(42)	-0.0562 (8)	0.113 (2)	0.1953 (8)	5.9 (4)*
C(43)	0.165 (1)	0.092 (2)	0.4349 (9)	7.7 (5)*
C(44)	0.121 (1)	0.135 (3)	0.482 (1)	9.8 (5)*
B	0.3521 (7)	0.103 (2)	0.0807 (7)	2.3 (3)*

^aStarred values denote atoms refined isotropically. Anisotropically refined atoms are given in the form of the isotropic equivalent displacement parameter defined as 8π²(U₁₁ + U₂₂ + U₃₃)/3.

Table III. Positional Parameters for [HB(Me₂pz)₃]MoO₂[S₂P(OEt)₂]^a

atom	x	y	z	B _{eq} , Å ²
Mo	0.21389 (5)	0.03822 (3)	0.18815 (3)	2.380 (9)
S(1)	0.0229 (2)	0.2135 (1)	0.24627 (9)	3.23 (3)
S(2)	-0.1053 (3)	0.4715 (1)	0.1885 (1)	5.76 (5)
P	0.0318 (2)	0.3283 (1)	0.1487 (1)	3.38 (3)
O(1)	0.1680 (4)	0.0414 (3)	0.0836 (2)	3.52 (9)
O(2)	0.3929 (4)	0.0782 (3)	0.1747 (3)	3.55 (8)
O(41)	0.2165 (5)	0.3247 (3)	0.1115 (3)	4.7 (1)
O(42)	-0.0217 (6)	0.2795 (3)	0.0669 (3)	5.0 (1)
N(11)	0.2429 (5)	0.0085 (3)	0.3374 (3)	2.95 (9)
N(12)	0.1972 (5)	-0.0767 (3)	0.3840 (3)	2.85 (9)
N(21)	-0.0112 (5)	-0.0305 (3)	0.2354 (3)	2.79 (9)
N(22)	-0.0041 (5)	-0.1169 (3)	0.2926 (3)	2.83 (9)
N(31)	0.3352 (5)	-0.1353 (3)	0.1888 (3)	2.71 (9)
N(32)	0.3013 (5)	-0.2053 (3)	0.2558 (3)	3.0 (1)
C(11)	0.3022 (7)	0.0614 (5)	0.3939 (4)	3.5 (1)
C(12)	0.2890 (7)	0.0117 (5)	0.4775 (4)	4.2 (1)
C(13)	0.2243 (7)	-0.0746 (5)	0.4681 (4)	3.6 (1)
C(14)	0.3695 (8)	0.1574 (5)	0.3697 (5)	5.0 (2)
C(15)	0.1832 (9)	-0.1545 (6)	0.5373 (4)	5.4 (2)
C(21)	-0.1610 (6)	-0.0075 (5)	0.2077 (4)	3.3 (1)
C(22)	-0.2502 (6)	-0.0782 (5)	0.2492 (4)	3.8 (1)
C(23)	-0.1474 (6)	-0.1481 (4)	0.3007 (4)	3.4 (1)
C(24)	-0.2151 (7)	0.0797 (5)	0.1408 (4)	4.7 (1)
C(25)	-0.1756 (8)	-0.2437 (5)	0.3558 (5)	5.3 (2)
C(31)	0.4669 (6)	-0.1915 (4)	0.1321 (4)	3.1 (1)
C(32)	0.5182 (8)	-0.2979 (5)	0.1623 (4)	4.2 (1)
C(33)	0.4115 (7)	-0.3038 (5)	0.2405 (4)	3.8 (1)
C(34)	0.5381 (8)	-0.1397 (5)	0.0516 (4)	4.4 (1)
C(35)	0.411 (1)	-0.3993 (6)	0.3014 (5)	6.4 (2)
C(41)	0.314 (1)	0.3722 (8)	0.1579 (6)	7.3 (2)
C(42)	0.463 (1)	0.3883 (8)	0.1027 (7)	9.3 (3)
C(43)	-0.040 (1)	0.3352 (7)	-0.0146 (5)	6.9 (2)
C(44)	-0.083 (1)	0.2686 (8)	-0.0777 (5)	7.8 (2)
B	0.1559 (8)	-0.1660 (5)	0.3327 (4)	3.1 (1)

^aAnisotropically refined atoms are given in the form of the isotropic equivalent displacement parameter defined as 8π²(U₁₁ + U₂₂ + U₃₃)/3.

(18) Jowitt, R. N.; Mitchell, P. C. H. *J. Chem. Soc. A* **1969**, 2632-2636.

(19) Chen, G. J.-J.; McDonald, J. W.; Newton, W. E. *Inorg. Chem.* **1976**, *15*, 2612-2615.

related $\{\text{HB}(\text{Me}_2\text{pz})_3\}\text{MoO}(\text{S}_2\text{CNR}_2)$ complexes from $\text{MoO}(\text{S}_2\text{CNR}_2)_2$ and $\text{K}\{\text{HB}(\text{Me}_2\text{pz})_3\}$.⁹

Compounds **1a** and **2** can be prepared simultaneously by the reaction of the binuclear Mo(V) complex $\text{Mo}_2\text{O}_3[\text{S}_2\text{P}(\text{OEt})_2]_4$ with $\text{K}\{\text{HB}(\text{Me}_2\text{pz})_3\}$ in toluene at 60 °C (eq 4). In solution, $\text{Mo}_2\text{O}_3[\text{S}_2\text{P}(\text{OEt})_2]_4 + 2\text{K}\{\text{HB}(\text{Me}_2\text{pz})_3\} \rightarrow \mathbf{1a} + \mathbf{2} + 2\text{K}\{\text{S}_2\text{P}(\text{OEt})_2\}$ (4)

$\text{Mo}_2\text{O}_3[\text{S}_2\text{P}(\text{OEt})_2]_4$ is known to participate in the equilibrium shown in eq 5.²⁰ The mononuclear disproportionation products $\text{Mo}_2\text{O}_3[\text{S}_2\text{P}(\text{OEt})_2]_4 \rightleftharpoons \text{cis-MoO}_2[\text{S}_2\text{P}(\text{OEt})_2]_2 + \text{MoO}[\text{S}_2\text{P}(\text{OEt})_2]_2$ (5)

are thought to be directly involved in the substitution reactions that lead to the formation of **1a** and **2**. This is supported by the reaction of $\text{MoO}[\text{S}_2\text{P}(\text{OEt})_2]_2$ with $\text{K}\{\text{HB}(\text{Me}_2\text{pz})_3\}$, which produces high yields of **1a**. Interestingly, however, the Mo(VI) complex $\text{MoO}_2[\text{S}_2\text{P}(\text{OEt})_2]_2$ has never been isolated and the formation of **2** may result from the reaction of $\text{K}\{\text{HB}(\text{Me}_2\text{pz})_3\}$ with a species produced by the decomposition of $\text{MoO}_2[\text{S}_2\text{P}(\text{OEt})_2]_2$. Solid **2** is stable in air, except for the slow loss of solvent of crystallization. In solution, however, **2** decomposes in a few days or weeks depending upon the solvent. Attempts to prepare the methyl analogue of **2** have consistently failed. When $\text{Mo}_2\text{O}_3[\text{S}_2\text{P}(\text{OMe})_2]_4$ is used in reaction 5, only **1b** is obtained.

The Mo(V) dithiocarbamate complexes $\text{Mo}_2\text{O}_3(\text{S}_2\text{CNR}_2)_4$ are also known to participate in an equilibrium analogous to that shown in eq 5. It is therefore conceivable that $\{\text{HB}(\text{Me}_2\text{pz})_3\}\text{MoO}(\text{S}_2\text{CNR}_2)$ and $\{\text{HB}(\text{Me}_2\text{pz})_3\}\text{MoO}_2(\eta^1\text{-S}_2\text{CNR}_2)$ could be prepared from the reaction of $\text{Mo}_2\text{O}_3(\text{S}_2\text{CNR}_2)_4$ and $\text{K}\{\text{HB}(\text{Me}_2\text{pz})_3\}$. However, in refluxing toluene this reaction yields $\{\text{HB}(\text{Me}_2\text{pz})_3\}\text{MoO}(\text{S}_2\text{CNET}_2)$ along with a number of byproducts, including $\text{Mo}_2\text{O}_2(\mu\text{-S})_2(\text{S}_2\text{CNET}_2)_2$, which precipitates from the reaction mixture. There is no evidence for the formation of $\{\text{HB}(\text{Me}_2\text{pz})_3\}\text{MoO}_2(\text{S}_2\text{CNET}_2)$, and separate experiments involving the reaction of $\text{MoO}_2(\text{S}_2\text{CNET}_2)_2$ with either $\text{K}\{\text{HB}(\text{Me}_2\text{pz})_3\}$ or $\text{NaS}_2\text{CNET}_2$ in refluxing toluene led to reduction, through intermediate purple and red stages, and the precipitation of $\text{Mo}_2\text{O}_2(\mu\text{-S})_2(\text{S}_2\text{CNR}_2)_2$. We believe that any $\text{MoO}_2(\text{S}_2\text{CNET}_2)_2$ formed in the disproportionation reaction analogous to eq 5 is rapidly reduced (by $\text{HB}(\text{Me}_2\text{pz})_3^-$ or $\text{S}_2\text{CNET}_2^-$) to $\text{MoO}(\text{S}_2\text{CNET}_2)_2$, which then forms $\{\text{HB}(\text{Me}_2\text{pz})_3\}\text{MoO}(\text{S}_2\text{CNET}_2)$ in the presence of excess $\text{HB}(\text{Me}_2\text{pz})_3^-$. Thus, the use of 2 equiv of $\text{K}\{\text{HB}(\text{Me}_2\text{pz})_3\}$ in its reaction with $\text{Mo}_2\text{O}_3(\text{S}_2\text{CNET}_2)_2$ results in greater than a 100% yield of $\{\text{HB}(\text{Me}_2\text{pz})_3\}\text{MoO}(\text{S}_2\text{CNET}_2)$ based on the amount of $\text{MoO}(\text{S}_2\text{CNET}_2)_2$ available from the disproportionation reaction (5) alone. We have recently described⁹ a high-yield synthesis of the complexes $\{\text{HB}(\text{Me}_2\text{pz})_3\}\text{MoO}(\text{S}_2\text{CNR}_2)$ by the reaction of $\text{K}\{\text{HB}(\text{Me}_2\text{pz})_3\}$ with $\text{MoO}(\text{S}_2\text{CNR}_2)_2$, which may be formed in situ from the reaction of $\text{MoO}_2(\text{S}_2\text{CNET}_2)_2$ or $\text{Mo}_2\text{O}_3(\text{S}_2\text{CNR}_2)_4$ and PPh_3 .

Our inability to isolate $\{\text{HB}(\text{Me}_2\text{pz})_3\}\text{MoO}_2(\text{S}_2\text{CNR}_2)$ may be related to two factors. First and most important, the rapid reduction of $\text{MoO}_2(\text{S}_2\text{CNET}_2)_2$ effectively prevents the formation of $\{\text{HB}(\text{Me}_2\text{pz})_3\}\text{MoO}_2(\text{S}_2\text{CNR}_2)$ by destroying the required precursor. Second, although dithiocarbamate ligands are particularly good at stabilizing metals in high oxidation states, the stabilization of a dioxo-Mo(VI) moiety by a η^1 -dithiocarbamate ligand is unlikely. Only a few η^1 -dithiocarbamate complexes are known for the group VI metals, and none of these complexes possess a metal in an oxidation state greater than 3.²¹ In contrast, η^1 -dithiophosphate ligands are found in Mo complexes of oxidation states of 5^{22,23} and 6 (**2**, this work). On steric grounds as well,

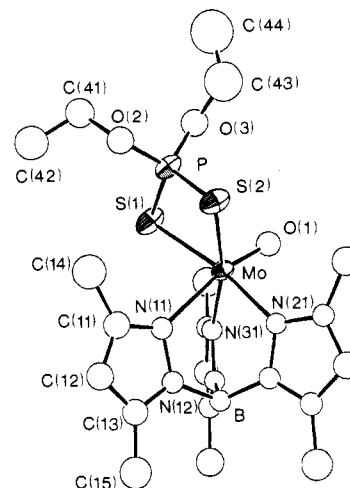


Figure 1. View of $\{\text{HB}(\text{Me}_2\text{pz})_3\}\text{MoO}[\text{S}_2\text{P}(\text{OEt})_2]$ (**1a**) showing the molecular structure and labeling scheme. Hydrogen atoms are omitted for clarity. Pyrazole rings are labeled such that the first digit following the atomic symbol refers to the ring containing that atom and the second digit is a sequence number assigned in the same manner for all rings.

Table IV. Selected Bond Distances (Å) and Angles (deg) in **1a** and **2**

$\{\text{HB}(\text{Me}_2\text{pz})_3\}\text{MoO}[\text{S}_2\text{P}(\text{OEt})_2]$ (1a)			
Mo-S(1)	2.478 (3)	Mo-N(21)	2.179 (7)
Mo-S(2)	2.500 (3)	Mo-N(31)	2.167 (7)
Mo-O(1)	1.644 (6)	S(1)-P	1.993 (4)
Mo-N(11)	2.452 (7)	S(2)-P	1.984 (4)
S(1)-Mo-S(2)	79.89 (9)	O(1)-Mo-N(11)	168.4 (2)
S(1)-Mo-O(1)	100.5 (2)	O(1)-Mo-N(21)	92.9 (3)
S(1)-Mo-N(11)	89.1 (2)	O(1)-Mo-N(31)	93.5 (3)
S(1)-Mo-N(21)	166.6 (2)	N(11)-Mo-N(21)	77.7 (3)
S(1)-Mo-N(31)	93.3 (2)	N(11)-Mo-N(31)	79.3 (3)
S(2)-Mo-O(1)	98.7 (2)	N(21)-Mo-N(31)	87.2 (3)
S(2)-Mo-N(11)	89.4 (2)	Mo-S(1)-P	84.7 (1)
S(2)-Mo-N(21)	96.9 (2)	Mo-S(2)-P	84.4 (1)
S(2)-Mo-N(31)	166.9 (2)	S(1)-P-S(2)	107.0 (2)
$\{\text{HB}(\text{Me}_2\text{pz})_3\}\text{MoO}_2[\text{S}_2\text{P}(\text{OEt})_2]$ (2)			
Mo-S(1)	2.468 (1)	Mo-N(31)	2.160 (2)
Mo-O(1)	1.690 (2)	Mo-S(2)	5.42
Mo-O(2)	1.697 (2)	S(1)-P(1)	2.047 (1)
Mo-N(11)	2.331 (2)	S(2)-P(1)	1.931 (1)
Mo-N(21)	2.302 (2)		
S(1)-Mo-O(1)	100.40 (8)	O(2)-Mo-N(11)	87.7 (1)
S(1)-Mo-O(2)	97.55 (8)	O(2)-Mo-N(21)	167.36 (9)
S(1)-Mo-N(11)	82.31 (6)	O(2)-Mo-N(31)	95.3 (1)
S(1)-Mo-N(21)	83.76 (7)	N(11)-Mo-N(21)	79.95 (9)
S(1)-Mo-N(31)	156.38 (7)	N(11)-Mo-N(31)	78.46 (9)
O(1)-Mo-O(2)	103.4 (1)	N(21)-Mo-N(31)	79.52 (9)
O(1)-Mo-N(11)	168.0 (1)	Mo-S(1)-P(1)	107.16 (4)
O(1)-Mo-N(21)	88.7 (1)	S(1)-P(1)-S(2)	111.06 (6)
O(1)-Mo-N(31)	95.8 (1)		

the stability of η^1 -dithiophosphate complexes is likely to be greater than that of analogous dithiocarbamate complexes due to the relative flexibility of the former compared to the rigidity of the latter.

Although we have prepared an extensive series of monomeric oxo-Mo(V) complexes using the $\text{HB}(\text{Me}_2\text{pz})_3^-$ ligand, we have been unable to isolate the cationic Mo(V) dithiophosphate complex $[\{\text{HB}(\text{Me}_2\text{pz})_3\}\text{MoO}[\text{S}_2\text{P}(\text{OEt})_2]]^+$. Attempts to prepare this complex via ligand substitution reactions of $\{\text{HB}(\text{Me}_2\text{pz})_3\}\text{MoOCl}_2$ lead only to **2** or to a disulfide-bridged dimer.²⁴ Attempts to oxidize **1a** via various one-electron chemical oxidants have not led to identifiable products, but we have obtained evidence for

(20) Chen, G. J.-J.; McDonald, J. W.; Newton, W. E. *Inorg. Nucl. Chem. Lett.* **1976**, *12*, 697-702.

(21) Young, C. G.; Roberts, S. A.; Enemark, J. H. *Inorg. Chem.* **1986**, *25*, 2667-2671. Young, C. G.; Roberts, S. A.; Enemark, J. H. *Inorg. Chim. Acta* **1986**, *114*, L7-L8 and references therein.

(22) Noble, M. E.; Huffman, J. C.; Wentworth, R. A. D. *Inorg. Chem.* **1982**, *21*, 2101-2103.

(23) Wall, K. L.; Folting, K.; Huffman, J. C.; Wentworth, R. A. D. *Inorg. Chim. Acta* **1984**, *86*, L25-27.

(24) Attempts to prepare the complex $[\{\text{HB}(\text{Me}_2\text{pz})_3\}\text{MoOCl}[\text{S}_2\text{P}(\text{OEt})_2]]^+$ led to the isolation of $\{\text{HB}(\text{Me}_2\text{pz})_3\}\text{MoO}(\mu\text{-S}_2)\text{MoO}[\text{HB}(\text{Me}_2\text{pz})_3]$. For details see: Roberts, S. A.; Young, C. G.; Cleland, W. E.; Yamanouchi, K.; Ortega, R. B.; Enemark, J. H. *Inorg. Chem.* **1988**, *27*, 2647.

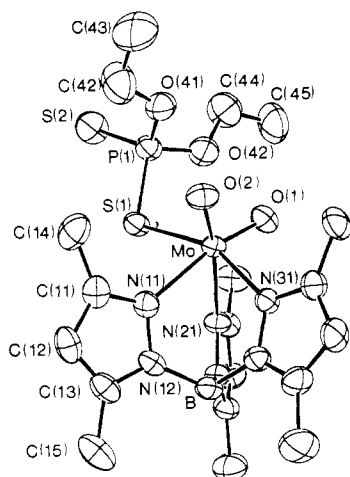


Figure 2. View of $\{\text{HB}(\text{Me}_2\text{pz})_3\}\text{MoO}_2\{\text{S}_2\text{P}(\text{OEt})_2\}$ (**2**) showing the molecular structure and labeling scheme. Hydrogen atoms are omitted for clarity. Pyrazole rings are labeled such that the first digit following the atomic symbol refers to the ring containing that atom and the second digit is a sequence number assigned in the same manner for all rings.

the formation of this cationic complex in solution during coulometry experiments (see below).

Description of the Structures. $\{\text{HB}(\text{Me}_2\text{pz})_3\}\text{MoO}\{\text{S}_2\text{P}(\text{OEt})_2\}$ (**1a**). A view of the structure of the $\{\text{HB}(\text{Me}_2\text{pz})_3\}\text{MoO}\{\text{S}_2\text{P}(\text{OEt})_2\}$ molecule along with the atomic labeling scheme used in the crystal structure determination is shown in Figure 1. Selected bond distances and angles are given in Table IV. The central molybdenum atom is bonded to one oxo group, two sulfur atoms from the bidentate $\text{S}_2\text{P}(\text{OEt})_2^-$ ligand, and three nitrogen atoms of the $\text{HB}(\text{Me}_2\text{pz})_3^-$ ligand. As usual, the pyrazolylborate ligand adopts *fac* coordination, leaving the $\text{Mo}=\text{O}$ and two $\text{Mo}-\text{S}$ bonds mutually *cis*. The $\text{Mo}=\text{O}$ bond length of 1.644 (6) Å is slightly shorter than the median distance of known $\text{Mo}^{\text{IV}}=\text{O}$ bonds (1.67 Å).⁹ A strong trans influence exerted by the $\text{Mo}=\text{O}$ fragment lengthens the $\text{Mo}-\text{N}(11)$ bond by ca. 0.28 Å compared to the $\text{Mo}-\text{N}(21)$ and $\text{Mo}-\text{N}(31)$ bonds *cis* to the $\text{Mo}=\text{O}$ bond. The dissociation of the trans N(11) atom to form a square-pyramidal five-coordinate complex is prevented by the tripodal coordination of $\text{HB}(\text{Me}_2\text{pz})_3^-$. The $\text{Mo}-\text{S}$ distances of 2.478 (3) and 2.500 (3) Å are in the expected range for such bonds.²² The bond distances in the pyrazolylborate ligand and the dithiophosphate ligand are normal.^{25,26} The coordination geometries in this complex and $\{\text{HB}(\text{Me}_2\text{pz})_3\}\text{MoO}(\text{S}_2\text{CNET}_2)$ ⁹ are remarkably similar, the major difference being the length of the $\text{Mo}=\text{O}$ bond, which is a normal 1.669 (4) Å in the dithiocarbamate complex. Even the extent of the trans influence of the $\text{Mo}=\text{O}$ bond is identical in the two structures.

$\{\text{HB}(\text{Me}_2\text{pz})_3\}\text{MoO}_2\{\text{S}_2\text{P}(\text{OEt})_2\}$ (**2**). The structure of $\{\text{HB}(\text{Me}_2\text{pz})_3\}\text{MoO}_2\{\text{S}_2\text{P}(\text{OEt})_2\}$ along with the atom-labeling scheme used in the structure determination is shown in Figure 2. Selected bond distances and angles are given in Table IV. The $\text{HB}(\text{Me}_2\text{pz})_3^-$ ligand adopts its usual facial coordination to the central molybdenum atom, leaving the two oxo groups and the sulfur of the monodentate dithiophosphate ligand mutually *cis*. Bond distances to the oxo ligands are normal²⁷ ($\text{Mo}=\text{O}(1) = 1.690$ (2) Å; $\text{Mo}=\text{O}(2) = 1.697$ (2) Å), as is the distance to the coordinated sulfur²² ($\text{Mo}-\text{S}(1) = 2.468$ (1) Å). The oxo ligands, as expected, exert a strong trans influence on the $\text{Mo}-\text{N}(11)$ (2.331 (2) Å) and $\text{Mo}-\text{N}(21)$ (2.302 (2) Å) bonds, lengthening them significantly with respect to the N(31) bond (2.160 (2) Å) trans to S(1). With the O(1)-Mo-O(2) angle being 103.4°, the overall geometry of the $\{\text{HB}(\text{Me}_2\text{pz})_3\}\text{MoO}_2$ fragment is the same, within experi-

mental error, as that of the μ -oxo dimer $\{\{\text{HB}(\text{Me}_2\text{pz})_3\}\text{MoO}_2\}_2\text{O}^{27}$. Bond distances and angles in the $\text{HB}(\text{Me}_2\text{pz})_3^-$ ligand and the monodentate dithiophosphate ligand are similar to those in previously reported structures.^{22,25}

The monodentate dithiophosphate ligand adopts an extended configuration, positioning the uncoordinated S(2) atom distal to and at a distance of 5.42 Å from the molybdenum. The P(1)-S(2) bond distance is significantly shorter than that of P(1)-S(1), a reflection of double-bond character. Although spatially extended, the $\text{S}_2\text{P}(\text{OEt})_2^-$ ligands are not involved in any close Mo-S(2) interactions within the lattice. This conformation of the $\text{S}_2\text{P}(\text{OEt})_2^-$ ligand contrasts with that of the $\eta^1\text{-S}_2\text{CNET}_2^-$ ligand of $\{\text{HB}(\text{Me}_2\text{pz})_3\}\text{Mo}(\text{S}_2\text{CNET}_2)_2$,²¹ where the uncoordinated sulfur of the monodentate dithiocarbamate ligand lies 3.8 Å from the molybdenum, capping a SNN face of the coordination sphere. The adoption of the extended configuration by **1a** could be dictated by steric effects since a proximal configuration of the $\eta^1\text{-S}_2\text{P}(\text{OEt})_2^-$ ligand is disfavored due to close contacts between its ethoxy groups and the 3-methyl groups of the $\text{HB}(\text{Me}_2\text{pz})_3^-$ ligand.

In addition to these steric effects, other factors may be important. While $\eta^1\text{-S}_2\text{CNR}_2$ complexes adopt only the proximal configuration,^{21,28} $\eta^1\text{-S}_2\text{P}(\text{OR})_2$ complexes have been found to adopt both proximal²⁹ and extended configurations²³ in the solid state. For both ligands, the proximal form occurs when the complex is of a late transition metal such as Au, Pt, or Pd²⁸ or a relatively low-valent early transition metal such as W(II) or Mo(III).²¹ An extended configuration of $\eta^1\text{-S}_2\text{P}(\text{OR})_2$ has, to our knowledge, only been previously characterized in Mo(V) complexes containing an arylimido ligand that are isoelectronic with $[\text{MoO}]^{3+}$ complexes.²³ No $\eta^1\text{-S}_2\text{CNR}_2$ complexes of high-valent metals have yet been prepared; attempts to prepare such Mo(V) complexes analogous to the $\eta^1\text{-S}_2\text{P}(\text{OR})_2$ complexes resulted only in products containing $\eta^2\text{-S}_2\text{CNR}_2$ ligands.

Spectroscopy and Electrochemistry. The infrared spectra of **1a** and **1b** exhibit strong single bands due to $\nu(\text{Mo}=\text{O})$ at 962 and 956 cm^{-1} , respectively. Bands characteristic of the $\text{HB}(\text{Me}_2\text{pz})_3^-$ and $\text{S}_2\text{P}(\text{OR})_2^-$ ligands are also present. The ¹H NMR spectra of the complexes are consistent with molecular C_s symmetry in solution as indicated by the number and intensity of the $\text{HB}(\text{Me}_2\text{pz})_3^-$ ligand resonances. Due to the geometry about the phosphorus atom the OR groups of the $\text{S}_2\text{P}(\text{OR})_2^-$ ligands are inequivalent and two sets of resonances assignable to the R groups are present in the spectra. In **1a**, coupling is observed between the methylene protons and the phosphorus nucleus ($J(^1\text{H}-^{31}\text{P}) = 7.1$ Hz). The coupling is not resolved in the ³¹P NMR spectrum; a single ³¹P{¹H} NMR signal at δ 135.4 is observed for **1a**. The coupling of the methyl protons and the phosphorus nucleus in **1b** ($J(^1\text{H}-^{31}\text{P}) = 13.5$ Hz) is readily discerned in the ¹H NMR spectrum and results in a well-resolved septet ³¹P NMR signal at δ 136.97. The ³¹P resonances of **1a** and **1b** are considerably deshielded compared to that of **2**.

Complexes **1a** and **1b** exhibit ⁹⁵Mo resonances at δ 2950 ± 10 and 2930 ± 10, respectively. The chemical shifts are among the most deshielded observed for oxo-Mo(IV) complexes. The related complexes $\{\text{HB}(\text{Me}_2\text{pz})_3\}\text{MoO}(\text{S}_2\text{CNR}_2)$ exhibit resonances at δ 3000 while the complexes $\text{MoOCl}_2(\text{N}-\text{N})(\text{PPh}_2\text{Me})$ (N-N = phen, bpy) exhibit the most deshielded resonances known for oxo-Mo(IV) complexes (ca. δ 3170).³⁰ The large line widths observed for the resonances of **1a**, **1b**, and **2** are typical of oxo-Mo(IV) complexes.³⁰

(25) Lincoln, S.; Soong, S.-L.; Koch, S. A.; Sato, M.; Enemark, J. H. *Inorg. Chem.* **1985**, *24*, 1355-1359.

(26) Dilworth, J. R.; Zubieta, J. A. *J. Chem. Soc., Dalton Trans.* **1983**, 397-398.

(27) Barnhardt, K. M.; Enemark, J. H. *Acta Crystallogr., Sect. C: Cryst. Struct. Commun.* **1984**, *C40*, 1362-1364.

(28) Lin, J. B.; Chen, H. W.; Fackler, J. P. *Inorg. Chem.* **1978**, *17*, 394-401. Abrahamson, H. B.; Freeman, M. L.; Hossein, M. B.; van der Helm, D. *Inorg. Chem.* **1984**, *23*, 2286-2293. Ashworth, C. C.; Bailey, N. A.; Johnson, M.; McCleverty, J. A.; Morrison, N.; Tabbiner, B. *J. Chem. Soc., Chem. Commun.* **1976**, 743. Kubicki, M. M.; Kergoat, R.; Gomes de Lima, L. C.; Carrou, M.; Scordia, H.; Guerschais, J. E.; Haridon, D. *L. Inorg. Chim. Acta* **1985**, *104*, 191-196.

(29) Fackler, J. P.; Thompson, L. D.; Lin, J. B.; Stephenson, T. A.; Gould, R. O.; Alison, J. M. C.; Fraser, A. J. F. *Inorg. Chem.* **1982**, *21*, 2397-2403. McCleverty, J. A.; Kowalski, R. S. Z.; Bailey, N. A.; Mulvaney, R.; O'Leirigh, D. A. *J. Chem. Soc., Dalton Trans.* **1983**, 627-634.

(30) Young, C. G.; Enemark, J. H. *Inorg. Chem.* **1985**, *24*, 4416-4419.

Yellow, diamagnetic **2** crystallizes from toluene as the toluene hemisolvate. All characterization data were collected with use of this solvate. The infrared spectrum of **2** exhibits bands due to $\text{HB}(\text{Me}_2\text{pz})_3^-$ and $\eta^1\text{-S}_2\text{P}(\text{OEt})_2^-$ ligands ($\nu(\text{BH})$ 2548 cm^{-1}). A strong pair of IR bands characteristic of the *cis*-dioxomolybdenum(VI) fragment are observed at 900 and 933 cm^{-1} . The ^1H NMR spectrum of the complex is consistent with molecular C_s symmetry in solution. The mirror plane dictates the presence of six sets of equivalent protons in the $\text{HB}(\text{Me}_2\text{pz})_3^-$ ligand, and singlet resonances having the intensity ratio 3:6:3:6:3(1 + 2) may be assigned to these proton sets. Symmetry also dictates the inequivalence of the methylene protons (H_A and H_B) of the $\text{S}_2\text{P}(\text{OEt})_2^-$ ligand. The ABX_3 resonance characteristic of these protons is reduced to an AB resonance when decoupled from the $\text{S}_2\text{P}(\text{OEt})_2^-$ methyl protons (δ 1.4). The complex exhibits a singlet $^{31}\text{P}\{^1\text{H}\}$ NMR signal at δ 95.75. $^{31}\text{P}\text{-}^1\text{H}$ coupling could not be resolved in the ^{31}P NMR spectrum. The singlet ^{95}Mo NMR signal at δ 162 (340 Hz) from this complex is at the shielded end of the chemical shift range established for *cis*-dioxomolybdenum(VI) complexes.³¹

The visible spectrum of **1a** is typical of oxomolybdenum(IV) complexes. The first two d-d bands are observed at 638 ($\epsilon = 100$) and 342 nm ($\epsilon = 80$). Charge-transfer transitions obscure the third d-d transition. The yellow **2** shows only intense charge-transfer bands, the first of which peaks at 340 nm ($\epsilon = 6080$). Thus, the interconversion of **1a** and **2** may be followed by changes in absorbance at 638 nm.

The electrochemical properties of **1a** and **2** were examined by cyclic voltammetry at a glassy-carbon electrode over the potential range +1.2 to -1.3 V in acetonitrile solution. **1a** exhibits only a quasi-reversible oxidation at +0.60 V ($\Delta E_p = 100$ mV at a sweep rate of 100 mV/s; $i_a/i_c = 1.0$) presumably arising from the one-electron oxidation of Mo(IV) to Mo(V). Coulometry in CH_2Cl_2 confirms this as a one-electron oxidation. Upon electrochemical oxidation, the solution turns from blue to orange-pink and develops an EPR spectrum (CH_2Cl_2 solution: $g = 1.965$, $A(^{95,97}\text{Mo}) = 42.5$ G, $A(^{31}\text{P}) = 72.5$ G), suggesting that the cationic $[\{\text{HB}(\text{Me}_2\text{pz})_3\}\text{MoO}\{\text{S}_2\text{P}(\text{OEt})_2\}]^+$ complex is formed during electrochemical oxidation of **1a**.

Cyclic voltammetry of **2** showed two irreversible cathodic waves at -0.50 and -0.90 V as well as an irreversible anodic wave at +0.75 V. This behavior is typical of complexes possessing the $[\text{MoO}_2]^{2+}$ moiety. The apparent product of the reduction would be an $[\text{MoO}_2]^+$ species, known to be unstable.³² The oxidation wave at +0.75 V is presumably due to oxidation of the uncoordinated sulfur of the dithiophosphate group.

Oxygen Atom Transfer Reactions. Complexes **1a** and **2** have identical stoichiometry except for the additional oxo ligand in **2**. Oxo-transfer reactions, such as those described in the Introduction, would interconvert these complexes. As a test of this concept, reactions analogous to those in eq 1 and 2 were carried out with complexes **1a** and **2** as the molybdenum-containing reactants. Spectra taken during these reactions are shown in Figure 3.

Figure 3a shows spectra recorded during the reaction of **1a** with a large excess of Me_2SO at 40 °C. The absorption at 638 nm is due to **1a** and decreases with time as the charge-transfer band of **2** at 340 nm grows in. An isosbestic point is observed, and the reaction goes to completion. Figure 3b shows spectra recorded during the reaction of **2** with a 3-fold excess of Ph_3P at 40 °C. Here, the 638-nm band of $\{\text{HB}(\text{Me}_2\text{pz})_3\}\text{MoO}\{\text{S}_2\text{P}(\text{OEt})_2\}$ is growing as a function of time. The lack of a clean isosbestic point is due to the formation of a species that absorbs at 475 nm. The amount of this species formed is dependent upon sample history and appears to be due to a side reaction of **2** with Ph_3P . Thus, complexes **1a** and **2** undergo the reactions comprising the catalytic reaction cycle defined by eq 1 and 2.

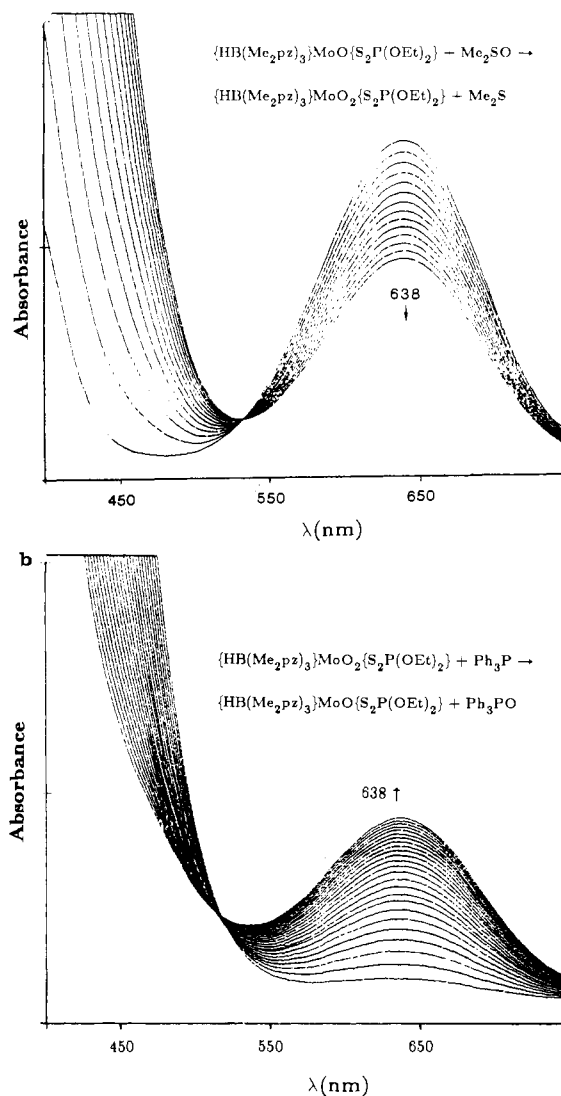
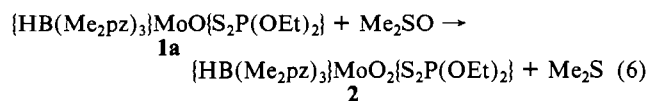


Figure 3. Optical absorption spectra taken during oxygen atom transfer reactions at 40 °C. (a) **1a** + excess Me_2SO , spectra taken every 20 min. The peak at 638 nm is diminishing in intensity. An isosbestic point is seen. (b) **2** + Ph_3P , spectra taken every 20 min. The peak at 638 nm is growing with time. No isosbestic point is observed; a second absorption near 475 nm appears that is not due to **1a** (see text).

Table V. Second-Order Rate Constants for the Reaction of **1a** with Me_2SO

solvent	T , °C	k , (M s^{-1}) ⁻¹
toluene	25	$1.51 (6) \times 10^{-5}$
	40	$5.46 (6) \times 10^{-5}$
	55	$1.73 (2) \times 10^{-4}$
	70	$5.15 (9) \times 10^{-4}$
MeCN	40	$4.3 (1) \times 10^{-5}$
	55	$1.83 (6) \times 10^{-4}$

Kinetic Studies. Oxygen Atom Transfer to $\{\text{HB}(\text{Me}_2\text{pz})_3\}\text{-MoO}\{\text{S}_2\text{P}(\text{OEt})_2\}$. The kinetics of the reaction shown in eq 6 were investigated in toluene under pseudo-first-order conditions by following the spectrophotometric disappearance of **1a** at 638 nm.



The reaction is first-order in molybdenum complex; plots of $\ln(A_0 - A_t)$ vs time are linear to at least 85% completion of the reaction. The reaction is also first-order in Me_2SO ; plots of $\ln k_{\text{obsd}}$ vs $[\text{Me}_2\text{SO}]_0$ at each temperature are straight lines with slopes of 1.0 ± 0.1 . The reaction follows a simple second-order rate law, $-d[\text{1a}]/dt = k[\text{1a}][\text{Me}_2\text{SO}]$. Plots of k_{obsd} vs $[\text{Me}_2\text{SO}]$, shown

(31) Minelli, M.; Yamanouchi, K.; Enemark, J. H.; Subramanian, P.; Kaul, B. B.; Spence, J. T. *Inorg. Chem.* **1984**, *23*, 2554-2556.

(32) Dowerah, D.; Spence, J. T.; Singh, R.; Wedd, A. G.; Wilson, G. L.; Farchione, F.; Enemark, J. H.; Kristofzski, J.; Bruck, M. *J. Am. Chem. Soc.* **1987**, *109*, 5655-5665.

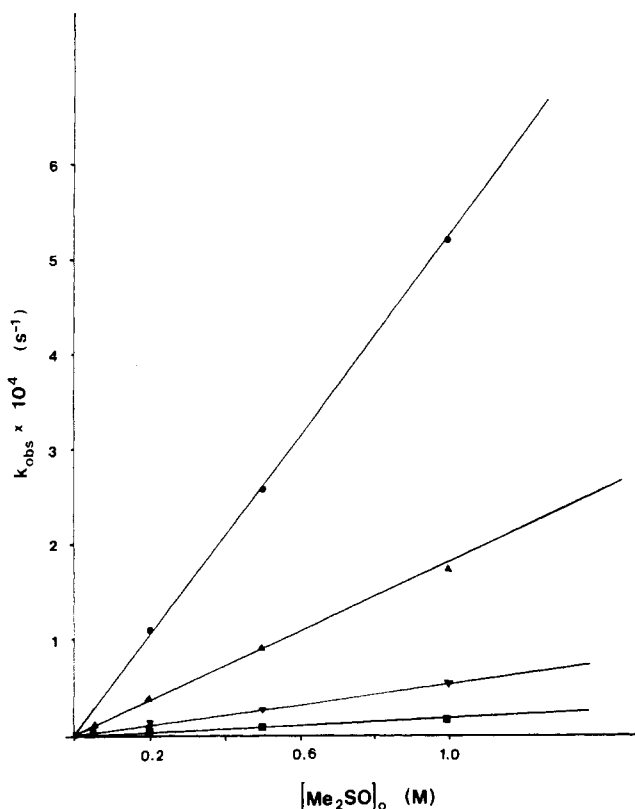


Figure 4. Plot of k_{obs} vs $[\text{Me}_2\text{SO}]_0$ for reaction 6: (●) 70 °C; (▲) 55 °C; (▼) 40 °C; (■) 25 °C.

in Figure 4, yield the second-order rate constant for the reaction (see Table V). From the Arrhenius plot, the following activation parameters have been determined: $\Delta H^\ddagger = 15.3$ (2) kcal mol⁻¹, $\Delta S^\ddagger = -29$ (2) cal (mol K)⁻¹.

Experiments were also run with MeCN as the solvent. Similar results were obtained, and these are also given in Table V. As can be seen from the data, there is only a slight solvent effect on the reaction.

The large negative ΔS^\ddagger coupled with the presence of a second-order rate implies an associative mechanism and the coordination of Me₂SO in the transition state. However, coordination of the Me₂SO molecule directly to **1a** is extremely unlikely. The starting Mo(IV) complex is already six-coordinate, and the steric bulk contributed by the 3-methyl groups of the HB(Me₂pz)₃⁻ ligand is known to effectively prevent seven-coordination of molybdenum complexes. A more reasonable first step in the reaction is cleavage of one of the Mo–S bonds of the $\eta^2\text{-S}_2\text{P}(\text{OEt})_2^-$ ligand to form a coordinatively unsaturated complex with an $\eta^1\text{-S}_2\text{P}(\text{OEt})_2^-$ ligand. A rapid preequilibrium between the $\eta^1\text{-}$ and $\eta^2\text{-S}_2\text{P}(\text{OEt})_2^-$ complexes prior to the rate-determining step of coordination of the oxygen atom of the Me₂SO molecule to the η^1 complex is consistent with the rate law. Concomitant oxo transfer from S to Mo would form **2**.

The second-order rate law for this reaction contrasts with that found for the reaction of the MoO(LNS₂) complex with Me₂SO,⁷ which shows saturation kinetics as generally observed for enzyme reactions. While our experiments were done at higher metal complex concentrations (3.5 vs 0.1 mM in ref 7), the $[\text{Me}_2\text{SO}]/[\text{Mo}(\text{IV})]$ ratios were comparable. In fact, for the reaction of **1a** with Me₂SO, the plot from which the rate constant was determined is linear at least to 1 M Me₂SO, a 200:1 $[\text{Me}_2\text{SO}]/[\text{Mo}(\text{IV})]$ ratio. In contrast, for the reaction of MoO(LNS₂) with Me₂SO, the same plot becomes nonlinear well before $[\text{Me}_2\text{SO}]$ reaches 0.01 M—a 100:1 ratio. The difference in kinetics behavior between the two systems is probably not due to the higher complex concentration used in these experiments. When the starting Mo complex is five-coordinate, as is the LNS₂ complex, the sixth coordination site can be occupied by either a solvent molecule or Me₂SO. Once the Me₂SO concentration is

sufficiently large, then all molecules have the sixth site occupied by the substrate; the rate of reaction becomes independent of $[\text{Me}_2\text{SO}]$, and saturation kinetics are observed. In the case of **1a**, this precomplexation by the substrate cannot occur because the initial complex is six-coordinate. Coordination of Me₂SO can occur only upon dissociation of one arm of the $\eta^2\text{-S}_2\text{P}(\text{OEt})_2^-$ ligand.

Interestingly, the corresponding Mo(IV) dithiocarbamate complex $\{\text{HB}(\text{Me}_2\text{pz})_3\}\text{MoO}(\text{S}_2\text{CNET}_2)$ ⁸ does not react with Me₂SO. Even in neat Me₂SO over a 48-h period no change in the spectrum of the complex occurs. We believe that the small bite angle, rigidity, and extensive π -delocalization of the MoS₂CN fragment may account for the stability of $\{\text{HB}(\text{Me}_2\text{pz})_3\}\text{MoO}(\text{S}_2\text{CNR}_2)$ by preventing the dissociation of a sulfur donor atom, proposed to be the first step in the reaction of **1a** and Me₂SO.

Oxygen Atom Transfer from $\{\text{HB}(\text{Me}_2\text{pz})_3\}\text{MoO}_2\{\text{S}_2\text{P}(\text{OEt})_2\}$. The kinetics of the reaction shown in eq 7 were investigated under pseudo-first-order conditions with Ph₃P in excess by monitoring the appearance of the 638-nm band of **1a**. With use of metho-

$$\{\text{HB}(\text{Me}_2\text{pz})_3\}\text{MoO}_2\{\text{S}_2\text{P}(\text{OEt})_2\} + \text{Ph}_3\text{P} \rightarrow$$

$$2 \{\text{HB}(\text{Me}_2\text{pz})_3\}\text{MoO}\{\text{S}_2\text{P}(\text{OEt})_2\} + \text{Ph}_3\text{PO} \quad (7)$$

1a

dology similar to that described above, the reaction was found to follow a second-order rate, $d[\mathbf{1a}]/dt = k[\mathbf{2}][\text{Ph}_3\text{P}]$. At 25 °C, $k = 3.4$ (1) × 10⁻³ (M s)⁻¹. Because of the limited solubility of **2** in toluene at lower temperatures and decomposition of the starting material in solution at higher temperatures reliable rate data could not be obtained at other temperatures.

All previous investigations of oxygen abstraction from Mo(VI) complexes by Ph₃P have found a second-order rate law.³³ The rate of reaction 7 is an order of magnitude smaller than that of MoO₂(S₂CNET₂)₂ with Ph₃P⁶ but the same order of magnitude as the reaction of Ph₃P with MoO₂(LNS₂).⁷

Oftentimes, oxygen abstraction with R₃P from MoO₂²⁺ complexes leads to formation of a Mo(V) dimer.⁶ The presence of the HB(Me₂pz)₃⁻ ligand appears to eliminate this side reaction. We have seen no evidence of dimer formation as the reaction proceeds, although there does seem to be degradation of the starting material, especially at higher temperatures. ³¹P NMR spectra of reaction mixtures in which a large excess of Ph₃P is reacted with **2** show that a small fraction of the Ph₃P has been converted to Ph₃PS (δ 42). This leads us to believe that the side reactions occurring include abstraction of sulfur from the dithiophosphate ligand by Ph₃P (and decomposition resulting therefrom) rather than dimerization of the complex. At higher temperatures this reaction proceeds readily, and by 55 °C, the oxygen abstraction reaction is no longer dominant.

Although we have observed oxo transfer to Ph₃P from $\{\text{HB}(\text{Me}_2\text{pz})_3\}\text{MoO}_2\text{X}$ (X = Cl⁻, Br⁻) complexes,³⁴ reaction 7 is the only one that yields an isolable monomeric Mo(IV) complex. For $\{\text{HB}(\text{Me}_2\text{pz})_3\}\text{MoO}_2\text{X}$ (X ≠ S₂P(OEt)₂⁻), the major product of the reaction with Ph₃P in chlorinated solvents is the Mo(V) complex $\{\text{HB}(\text{Me}_2\text{pz})_3\}\text{MoOClX}$. In other solvents, an as yet uncharacterized polynuclear complex is formed.

Catalysis of Oxo Transfer from Me₂SO to Ph₃P. Coupling of the reactions in eq 6 and 7 leads to a catalytic cycle⁷ resulting in a net oxygen atom transfer reaction from Me₂SO to Ph₃P. Both dithiophosphate complexes **1a** and **2** catalyze the reaction cycle, as shown by using ³¹P NMR to follow the conversion of a large excess of Ph₃P (δ -4.3) to Ph₃PO (δ 27.0). In the presence of either **1a** or **2** and excess Me₂SO, in 24 h at 40 °C under nitrogen, a 40-fold excess of Ph₃P is converted completely to the oxide and a small amount of Ph₃PS (as noted above). In the absence of the molybdenum complex, no reaction between Me₂SO and Ph₃P occurs under these conditions. Head-space analysis by GC/MS confirmed that Me₂S is formed as the other product of this reaction

(33) Holm, R. H. *Chem. Rev.* **1987**, *87*, 1401-1449.

(34) Young, C. G.; Roberts, S. A.; Cleland, W. E.; Enemark, J. H., manuscript in preparation.

cycle. Thus, both **1a** and **2** function as rudimentary chemical models for oxo-type molybdoenzymes, even though **1a** is coordinatively saturated.

Conclusions

The dithiophosphate complexes **1a** and **2** have been prepared and characterized by spectroscopic and crystallographic techniques. These six-coordinate complexes are further examples of oxo-Mo(IV) and dioxo-Mo(VI) complexes that undergo facile oxygen atom transfer reactions and catalyze the oxidation of PPh₃ by Me₂SO. The catalytic system described here employs the sterically encumbering HB(Me₂pz)₃⁻ ligand to prevent Mo(V) dimer formation. Kinetic studies of the oxygen atom transfer reaction of **1a** and Me₂SO are interpreted in terms of dissociation of one sulfur atom of the η²-dithiophosphate ligand to form an η¹-dithiophosphate complex prior to the transfer of an oxygen atom from Me₂SO to the Mo(IV) center. Oxygen atom transfer upon the nucleophilic attack of PPh₃ on the Mo(VI) center of **2** is followed by the rapid coordination of the second sulfur atom of the dithiophosphate ligand to form **1a**. As in previous systems^{6,7} the

coordination sphere of the Mo(VI) complex contains sulfur donor ligands. However, in contrast with previous systems^{5,7} in which oxygen atom transfer to the Mo(IV) complex is facilitated by the presence of vacant coordination sites or labile solvent ligands on the metal center, both **1a** and **2** are six-coordinate. This study demonstrates that oxygen atom transfer may also be facilitated by changes in the denticity of ligands bound to the metal center.

Acknowledgment. We gratefully acknowledge support of this work by the National Institutes of Health (Grant No. GM-37773). The structure determinations were done with use of the facilities of the Molecular Structure Laboratory, Department of Chemistry, University of Arizona. ³¹P NMR measurements were made by Dr. K. Christensen. GC/MS analyses were by M. Malcomson of the University Analytical Center of the University of Arizona.

Supplementary Material Available: Tables of anisotropic thermal parameters, calculated atomic positions, and bond distances and angles for {HB(Me₂pz)₃}MoO{S₂P(OEt)₂} and {HB(Me₂pz)₃}MoO₂{S₂P(OEt)₂}·0.5C₇H₈ (7 pages); tables of observed and calculated structure factors (28 pages). Ordering information is given on any current masthead page.

Notes

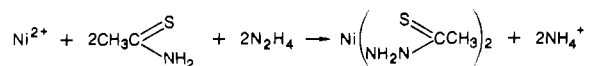
Contribution from the Department of Chemistry,
Royal Veterinary and Agricultural University,
DK-1871 Frederiksberg, Denmark,
and Department of Physical Chemistry,
H. C. Ørsted Institute, DK-2100 Copenhagen, Denmark

Structural Chemistry of Cobalt(III) Complexes of Thioacylhydrazide and Thioacylhydrazonate Ligands. Crystal Structures of (-)-D-*fac*-Tris(thioacetylhydrazide)cobalt(III) Chloride, (-)-D-*fac*-Tris(formaldehyde thioacetylhydrazidato)cobalt(III) Hydrate, and *fac*-Tris(thiosemicarbazide)cobalt(III) Chloride

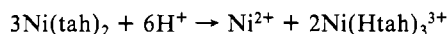
Erik Larsen,*¹ Sine Larsen,*² and Gitte Lunding¹

Received December 15, 1987

Thiosemicarbazide was found to be an excellent ligand for transition-metal ions by Jensen in 1934,³ and since then coordination compounds of thiosemicarbazide have been studied intensively.⁴ Simple thioacylhydrazides of aliphatic acids have been known for a few years, since they can be made by a metal ion assisted synthetic route. In the case of thioacetylhydrazide, the first step is the isolation of the sparingly soluble *trans*-bis(thioacetylhydrazidato)nickel(II), Ni(tah)₂.⁵

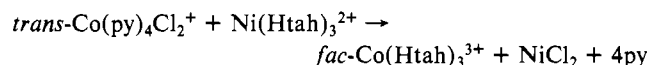


Bis(thioacetylhydrazidato)nickel(II) undergoes disproportionation on protonation with strong acids in water analogously to the behavior of the thiosemicarbazidato complex:⁶

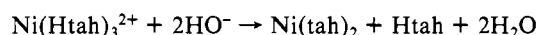


Tris(thioacetylhydrazide)nickel(II) chloride is easily isolated from the reaction mixture and may serve as a ligand donor to cobalt(III)

in the unstable *trans*-dichlorotetrakis(pyridine)cobalt(III) perchlorate:⁷

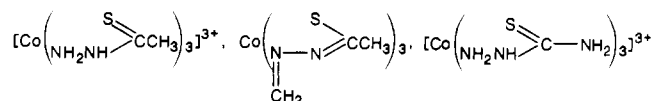


The free thioacetylhydrazide has been isolated according to the reaction scheme⁸



The formation of thiosemicarbazones and other hydrazones from the hydrazine derivative and an oxo compound is catalyzed by acid. It may therefore not be surprising that Ni(Htsc)₃²⁺ and Co(Htah)₃³⁺ react readily with aldehydes and ketones. In some cases it has even been possible to make coordination compounds of thioacylhydrazones that are otherwise unknown.^{9,10}

The present structure determinations were performed to obtain an understanding of the degree of delocalization in the three ligand systems



and to establish with certainty the absolute configuration of the two chiral coordination compounds.

Experimental Section

Preparation of Compounds. Δ-*fac*-(-)-D-Co(Htah)₃Cl₃ (I) was obtained according to published methods.⁷ Δ-*fac*-(-)-D-Co(CH₂=tah)₃·H₂O was prepared from this product. A 1.2-g amount of I was dissolved in hot water (12 mL), and after cooling to room temperature, 12 mL of 35% aqueous formaldehyde was added. The desired product precipitated during 5 h. *fac*-Co(Htsc)₃Cl₃ was obtained as described in the literature.¹¹ It has been reported to be isostructural with the rhodium complex.¹²

X-ray Crystallography. The three crystal structures were determined by the heavy-atom method and refined by least squares, minimizing Σw(|F_o| - |F_c|)². Table I contains a summary of the crystal data as well as some details for the data collection and structure refinements. The positional parameters for the non-hydrogen atoms in the structures are

- (1) Royal Veterinary and Agricultural University.
- (2) H. C. Ørsted Institute.
- (3) Jensen, K. A.; Rancke-Madsen, E. *Z. Anorg. Allg. Chem.* **1934**, *219*, 243.
- (4) Campbell, M. *Coord. Chem. Rev.* **1975**, *15*, 279.
- (5) Larsen, E.; Trinderup, P.; Olsen, B.; Watson, K. J. *Acta Chem. Scand.* **1970**, *24*, 261.
- (6) Jensen, K. A. *Z. Anorg. Allg. Chem.* **1934**, *221*, 6, 11.

- (7) Gabel, J.; Larsen, E. *Acta Chem. Scand., Ser. A* **1978**, *A32*, 929.
- (8) Jensen, K. A.; Larsen, E. *Acta Chem. Scand., Ser. A* **1979**, *A33*, 137.
- (9) Gabel, J.; Larsen, E. *Acta Chem. Scand., Ser. A* **1977**, *A31*, 657.
- (10) Gabel, J.; Haseman, V.; Henriksen, H.; Larsen, E.; Larsen, S. *Inorg. Chem.* **1979**, *18*, 1088.
- (11) Sun, K. K. W.; Haines, R. A. *Can. J. Chem.* **1970**, *48*, 2327.
- (12) Samus, I. D. *Koord. Khim.* **1981**, *7*, 120.